www.sciencemag.org/cgi/content/full/1178658/DC1

Supporting Online Material for

Character and Spatial Distribution of OH/H_2O on the Surface of the Moon Seen by M^3 on Chandrayaan-1

C. M. Pieters,* J. N. Goswami, R. N. Clark, M. Annadurai, J. Boardman, B. Buratti, J.-P. Combe, M. D. Dyar, R. Green, J. W. Head, C. Hibbitts, M. Hicks, P. Isaacson, R. Klima, G. Kramer, S. Kumar, E. Livo, S. Lundeen, E. Malaret, T. McCord, J. Mustard, J. Nettles, N. Petro, C. Runyon, M. Staid, J. Sunshine, L. A. Taylor, S. Tompkins, P. Varanasi

*To whom correspondence should be addressed. E-mail: carle_pieters@brown.edu

Published 24 September 2009 on *Science* Express
DOI: 10.1126/science.1178658

This PDF file includes:

1178658 Supporting Online Material

SOM Materials and Methods:

Description of M^3:

The Moon Mineralogy Mapper (M^3) is a NASA guest instrument on Chandrayaan-1, India's first mission to the Moon, which was launched successfully on October 22, 2008. The M^3 is designed to map the surface mineralogy of the Moon in geologic context at high spatial and spectral resolution using reflected solar radiation at near-infrared wavelengths (1). These data provide in depth information about geologic processes involved in the early crustal evolution of a silicate body in our Solar System. M^3 is a "push-broom" imaging spectrometer designed at full resolution to acquire 260 spectral channels from 430 to 3000 nm simultaneously for each of 600 cross-track spatial elements. Spacecraft motion provides the second dimension of spatial information, to build a three-dimensional cube of inherently co-registered spectra.

The first of four planned optical periods of Chandrayaan-1 operation extended through February 2009. Over this period, M^3 acquired near-infrared low-resolution spectra for ~60% of the lunar nearside (140 m/pixel; 85 spectral channels from 460 to 3000 nm) comprising more than a billion individual spectral measurements. All M^3 spectra in this manuscript were acquired in the M^3 low-resolution mode, which has only 25 spectral channels between 2000 and 3000 nm (instead of 100 spectral channels for M^3 full-resolution). With initial calibration, these M^3 data have proved to be of high quality and the instrument performed within specifications (*2*). Second order calibration steps, including in-flight calibrations and band-to-band corrections are ongoing and will continue to be refined. Lunar coordinates are assigned to each pixel. The M^3 overview hemispheric data-cube used for several illustrations was produced by reducing the spatial resolution by a factor of 100 to 1.4 km/pixel (*3*).

Thermal emission and lunar 3-μm band strength:

As discussed in the text and (4,5), a minor thermal emission component may exist beyond 2.6 μm under moderately strong solar illumination. Considerable variation of the 3-μm feature is observed to occur across local terrain with the high spatial resolution of M^3 data, and some local band weakening is likely due to small increases in thermal emission associated with local solar insolation variations due to topography. The science operation plan for M^3 was not originally designed to measure the lunar surface when it is cool (low solar illumination). Since the M^3 primary science goal is mapping lunar surface mineralogy (Fig 1D), science measurements typically require the maximum solar illumination for the best signal-to-noise ratio, and consequently a significant thermal emission component often occurs above 2000 nm at low latitudes (e.g. Fig. 1C and brown spectrum in Fig. 3A). With the recognition of the presence of a lunar 3-μm absorption, however, possible latitude-dependent issues raised by the new data should be resolved by comparing different illumination conditions (time of day) and thus different surface temperatures. We anticipate compositional and possibly temperature dependencies will affect the 3-μm absorption band shape and position and thus do not expect the current, limited suite of laboratory measurements to fully match observed lunar measurements.

SOM Supporting Text:

How dry is the Moon?

The search for water in returned lunar rocks and soils has been intensely studied. It has long been recognized that any water on the Moon or in Apollo samples may come from both endogenic and exogenic sources. Even the 'rust' [FeO(OH)] discovered in several Apollo 16 breccias has been attributed to the contamination by terrestrial air (*6,7*), although a cometary origin for the water has also been suggested (*8*). Water released from lunar soils was detected during early step-wise heating experiments (*9*). This water was largely attributed to terrestrial contamination, but also to possible reactions with solar wind-implanted protons in the soils. It was suggested that hydroxyl ions (OH^-) could form from the interaction of implanted solar wind with oxygen of minerals grains (10), and the process was verified experimentally (11). The paradigm for the formation of ubiquitous nanophase metallic Fe ($npFe^0$) observed in agglutinitic glass and vapor-deposited rims on soil grains is that solar wind implanted hydrogen reduces local FeO to metallic iron during micro-meteorite melting and vaporization of soil particles (*12*). If this reaction occurs, it should be accompanied by the production of water, some of which should remain in the quenched melt (and eventually agglutinitic glass). An early infrared spectroscopic examination of some of this agglutinitic glass, however, did not detect the presence of this hypothesized water (*13*). Recently, Saal et al. (*14*) have detected 20-45 ppm water in the interior of Apollo 15 green and Apollo 17 orange volcanic glasses, which are believed to be the most primitive materials from the lunar mantle in the sample collection, and this discovery sparked a new wave of sample analyses using modern laboratory equipment. Nevertheless, historically the Moon has been believed to be quite 'dry'.

Water on or in the lunar regolith is constrained by the harsh but variable lunar environment and the nature of lunar soil grains. Small amounts of water are regularly introduced into the lunar environment by the bombardment of water-bearing meteorites and meteoritic dust. It has been proposed that a few layers of molecular water could be thermodynamically stable (e.g. *15*) or that OH or H may simply exist as molecules adsorbed onto the regolith grains (*16,17*). It has also been demonstrated experimentally that water can adsorb onto surfaces either physically, retaining its integrity, or chemically (dissociatively) to form OH^-. Both single and multiple layers of different forms of OH and H_2O have been observed on simple mineral species along with the general temperature range of stability (*18*).

SOM FIGURES

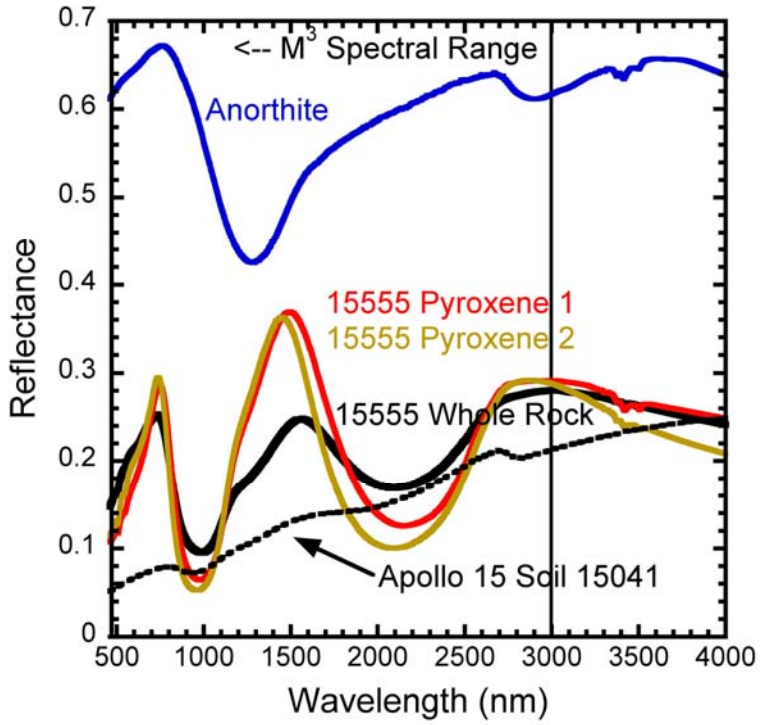

Fig. S1. Reflectance spectra of particulate lunar soil, rock, and minerals measured in Earth-based laboratory (RELAB). While plagioclase and pyroxene are the most abundant minerals on the Moon, the spectral properties of pyroxene often dominate near-infrared spectra of lunar rocks. Spectra of returned lunar soils measured in terrestrial controlled laboratory settings exhibit weaker diagnostic absorptions than local rocks due to space weathering. In the laboratory, soils also always exhibit a small absorption feature near 3-µm, while clean, coarse-grained lunar mineral separates or crushed rock often do not. The observed 3-µm features in laboratory reflectance spectra of particulate materials have been presumed to be due to residual terrestrial OH/H_2O adsorbed on soil grains. These features are weak, but remain when samples are placed overnight in a water-free environment for measurement and also when the samples are heated beyond lunar typical surface temperatures (*19, 20, 21)*. Weak features near 3400 nm are trace organic contaminants acquired during mineral processing. Although the physical properties (grain size, etc.) and processing and measurement history of the anorthite plagioclase mineral separate were identical to the others, it is observed to exhibit stronger features near 3-µm relative to other lunar mineral separates.

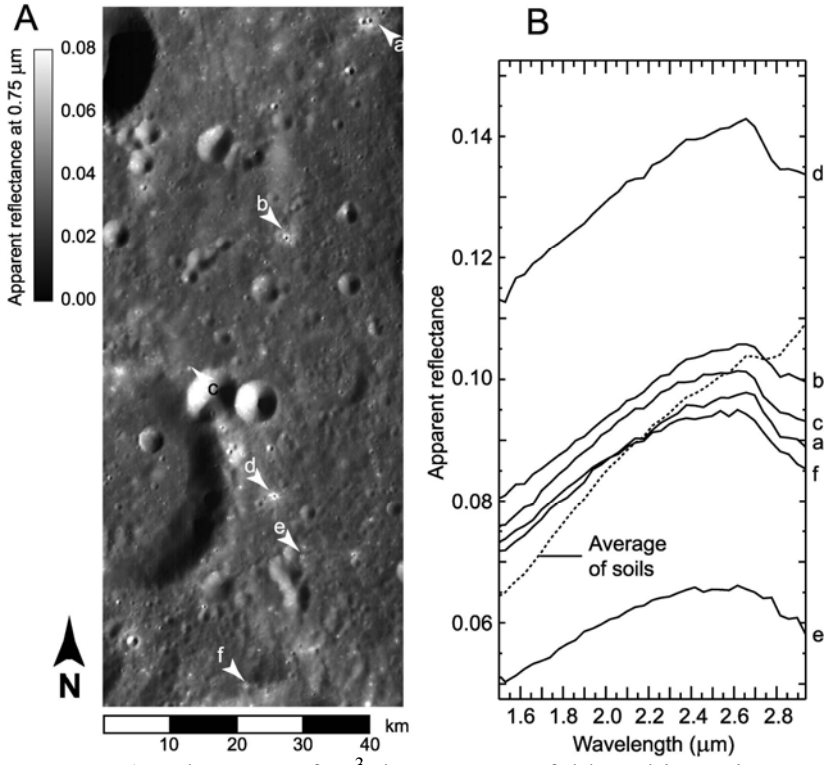

Fig. S2. A) Sub-scene of M^3 data across a feldspathic region north of Orientale on the farside centered near 33°N, 261°E. Arrows indicate the location of small morphologically fresh craters. B) M^3 near-infrared apparent reflectance spectra for the small fresh craters shown in A. Several 5x5 pixel regions of background soil have been collected and the average spectrum for background soil (dashed line) is shown for comparison. These data have been calibrated using M^3 radiance J-calibration with a 5-channel Gaussian filter applied for residual band-to-band deviations. Solar incidence geometry was low and these areas in the subscene exhibit no detectible thermal component. Although solar illumination effects exhibited elsewhere (Figs. 2, S3) are also common for this subscene, the small fresh feldspathic craters exhibit prominent 3-µm absorptions in comparison to their surroundings.

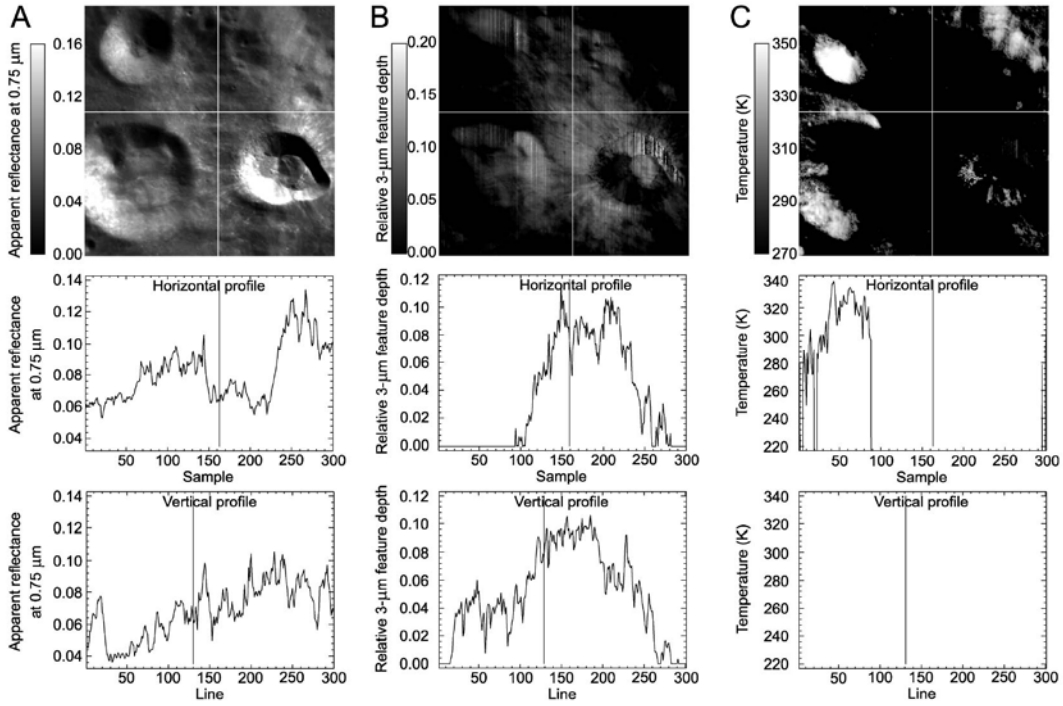

Fig. S3. Traverses across the subscene shown in Fig. 5. Along the top are (A) images of 750 nm brightness, (B) 3-µm relative band depth, and (C) derived temperature (black represents temperature below M3 detectable limit). The middle row presents data traverses along the horizontal profile and the bottom row presents data traverses along the vertical profile. The presence of a 3-µm absorption is clearly associated with the cool feldspathic ejecta of Ryder Crater. A generally inverse correlation of the 3-µm absorption with solar illumination (topography) for some of the data is apparent in the horizontal traverse, but not readily seen in the vertical.

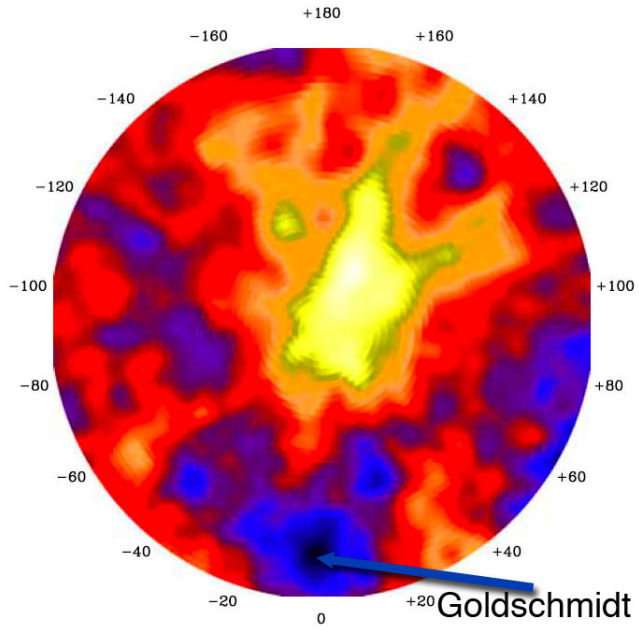

Fig. S4. Map of hydrogen abundance for the north pole northward of 70° derived from improved modeling of Lunar Prospector Neutron Spectrometer data (after Lawrence et al., *(22)*). High abundances are shown in yellow-white and approach 130-140 ppm regionally, but could exist as local concentrations much higher (several %) in permanently shadowed regions. Low abundances are shown in dark blue and average 5-10 ppm. Lawrence et al. estimate the average hydrogen abundance at latitudes lower than 70° to be ~50 ppm.

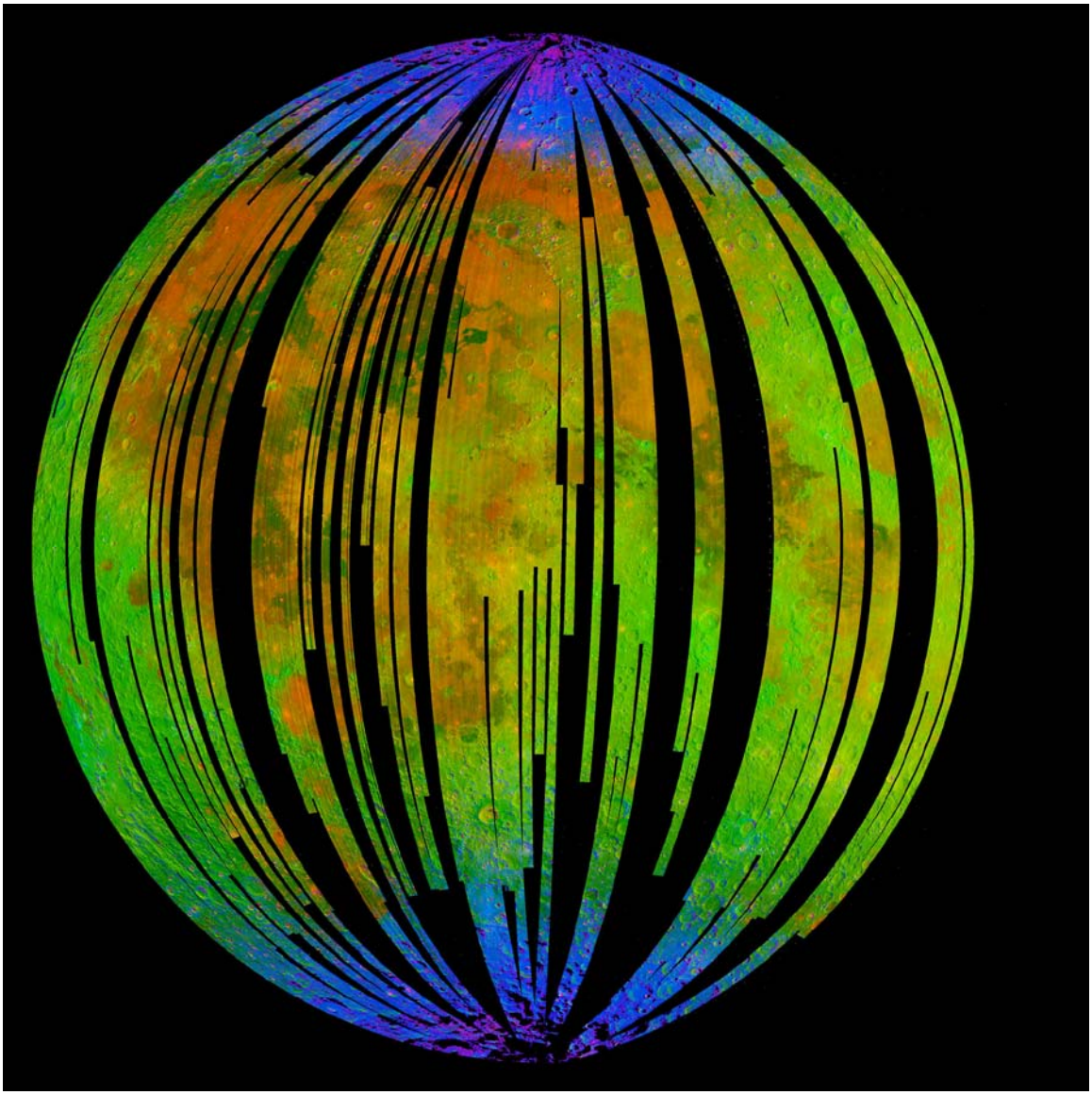

Fig. S5.A three-color composite of near-infrared reflected solar radiation for the lunar nearside illustrating the spatial extent of diagnostic absorptions measured by the Moon Mineralogy Mapper (M^3). Blue = 3-μm absorption associated with OH/H_2O, Green = reflected solar radiation (brightness) at 2.4-μm, and Red = absorption at 2-μm due to the presence of iron-bearing pyroxene. The presence of small amounts of OH/H_2O is detected as surficial materials and appears to be a function of the surface thermal and radiation environment and perhaps composition. During the time of day that is shown in this image, the detection of volatiles is most prominent at the higher, cooler latitudes. As the lunar day progresses, such conditions also extend to lower latitudes when the sun is lower in the lunar sky, but such cool equatorial conditions have not yet been analyzed by M^3.

References:

1. C. M. Pieters et al., *Current Science*, VOL. 96, NO. 4, 25 pp. 500-505 (Feb. 2009).
2. R. O. Green et al., 40th Lunar and Planetary Science Conference, Houston # 2307 (2009).
3. J.W. Boardman, et al., 6th EARSeL SIG IS workshop on Imaging Spectroscopy, Tel-Aviv, Israel (2009).
4. Clark, R. N., *Icarus*, 40, 94-103 (1979).
5. R. C. Clark, C. M. Pieters, R. O. Green, et al., 40th Lunar and Planetary Science Conference, Houston # 2136 (2009).
6. L.A.Taylor, H.-K. Mao, P.B. Bell, *Proc. 4th Lunar Sci. Conf., Geochim. Cosmochim. Acta*, 829-839, (1973).
7. L.A.Taylor, H.-K. Mao, P.B. Bell, *Proc. 5th Lunar Sci. Conf., vol. 1, Geochim. Cosmochim. Acta*, Suppl. 3, 743-748. (1974).
8. A. El Goresy et al. *Earth Planet. Sci. Lett. 18*, 411-419, (1973).
9. E. K. Gibson, S. M. Johnson, *Proc. Third Lunar Sci. Conf., Vol. 2, Geochim. Cosmochim. Acta*, The M.I.T. Press, 1351-1356 (1971).
10. E. J. Zeller, Dreschhoff, G., Kevan, L., *Modern Geology 1*, 141-148 (1970)
11. E. K. Gibson, Moore, G.W., *Proc. 3d Lunar Sci. Conf., Vol. 2, Geochim. Cosmochim. Acta*, The M.I.T. Press, 2029-2040 (1972).
12. R. M.Housley, R. W. Grant, N. E. Paton, Proc. 4th Lunar Sci. *Conf., Vol 3, Geochim. Cosmochim. Acta*, The M.I.T. Press, 2737-2749 (1973).
13. L. A. Taylor, G. R. Rossman, Q. Qi, Lunar & Planetary Science XXVI, Lunar and Planetary Institute, Houston, 1399-1400, (1995).
14. A. E. Saal et al., *Nature 454*, doi:10.1038, (2008).
15. F. H. Cocks et al., *Icarus*, 160, 386-397 (2002).
16. L. Starukhina, Y. Shkuratov, *Icarus*, 147, 585-587 (2000).
17. C. A. Hibbitts, M. D. Dyar, T.M. Orlando, G. Grieves, J. Szanyi, 40th Lunar and Planetary Science Conference, Houston, # 1926 (2009).
18. C. D. Lane, N. G. Petrik, T. M. Orlando and G. A. Kimmel, *J. Phys. Chem. C*, **111**, 16319 (2007).
19. C. M. Pieters, L. A. Taylor, *Lunar Planet. Sci. XXIX*, Houston, TX, pp. CD-ROM, Abstract #1840, (1998).
20. P. J. Isaacson, C. M. Pieters *Lunar Planet. Sci.* [CD-ROM], *XXXVIII*, abstract 2070 (2007).
21. P. J. Isaacson et al., 40th Lunar and Planetary Science Conference, Houston # 1821 (2009).
22. D. J. Lawrence et al., *J. Geophys. Res*. (Planets) 111, E08001, doi:10.1029/2005JE002637 (2006).